

Assessment of a Wigner-distribution-function-based method to compute the polychromatic axial response given by an aberrated optical system

Walter D. Furlan
Genaro Saavedra
Enrique Silvestre

Universitat de València
Departamento de Óptica
46100 Burjassot, Spain
E-mail: walter.furlan@uv.es

Juan A. Monsoriu

Universidad Politécnica de Valencia
Departamento de Física Aplicada
46022 Valencia Spain

José D. Patrignani

Universidad Nacional del Sur
Departamento de Física
8000 Bahía Blanca, Argentina

Abstract. A numerical method that uses the Wigner distribution function to compute the impulse response along the optical axis provided by an aberrated optical system is evaluated. The technique is compared with a classical method used to compute the response integral. Test systems with pupils of nonconventional shape are considered. It is shown that, in general, the same degree of accuracy for the computation of the polychromatic merit functions is achieved faster by use of this novel method. © 2003 Society of Photo-Optical Instrumentation Engineers. [DOI: 10.1117/1.1541003]

Subject terms: impulse response computation; Wigner distribution function; polychromatic merit functions; spherical aberration; square pupils; triangular pupils; elliptical pupils.

Paper 020193 received May 15, 2002; revised manuscript received Sep. 12, 2002; accepted for publication Sep. 12, 2002

1 Introduction

The performance of an aberrated optical system working under broadband illumination can not be properly evaluated using a single monochromatic merit function such as the point spread function (PSF) or the optical transfer function (OTF). A high number of monochromatic PSFs or OTFs must be considered instead. These monochromatic functions can be used to define the corresponding polychromatic merit function by the addition of all of them, weighted by the spectral distribution of the source and the color sensitivity of the receiver. The study of the polychromatic merit functions of a system along the optical axis is frequently used as a test of its tolerance to aberrations.^{1,2} In particular, for visual optical systems—i.e., those systems in which the human eye is the final detector—the classical merit functions are the tristimuli values along the optical axis. Since analytical expressions for the monochromatic irradiance PSFs are achievable only for a few pupils of simple shape, several numerical methods to evaluate them have been developed.^{3–6} All of them are based on the division of the pupil function into many subareas, and the subsequent addition of their contribution to the final image. Consequently, when numerical methods are used to calculate polychromatic merit functions, the sequential computation of many monochromatic PSFs leads to a time-consuming procedure.

A completely different approach to the computation of the diffraction integral for aberrated optical systems was recently proposed.⁷ It is based on the mathematical relationship between the irradiance at a given point in the image space, and the Wigner distribution function (WDF) obtained from the pupil function of the system. This method was extended to the polychromatic domain and demon-

strated to be especially useful for the computation of the polychromatic axial response provided by an optical system with an arbitrary exit pupil transmittance. Moreover, preliminary results showed that its efficiency is even better for systems suffering from longitudinal chromatic aberration (LCA) and spherical aberration⁸ (SA). In this case, a single phase-space function, namely, the WDF of the azimuthally averaged pupil function of the system, is enough to obtain the polychromatic response along the optical axis.

The purpose of this paper is to assess the performance of the new method, carrying out a systematic comparative study with an optimized version⁴ of the classical method of Hopkins and Yzuel. The choice of the test systems for the comparison was oriented toward recent novel applications that use optical systems with different kind of apertures. Specifically, a triangular aperture and a square aperture were considered. This kind of apertures has recently deserved the attention of scientists in different fields. Triangular apertures in unstable laser resonators produce diffraction patterns having interesting fractal behavior.⁹ On the other hand, square apertures have been recently proposed by the astronomers to reduce the diffraction lobes of the telescopic images, enabling detection of earth-like planets orbiting sun-like stars.¹⁰ It is shown here that our method enables an efficient analysis of such systems. Finally, elliptical pupils were also studied, since this kind of pupils must be considered when dealing with off-axis object points in systems with standard circular clear pupils.¹¹

2 Numerical Methods

Let us consider a general isoplanatic optical system designed to work under broadband illumination, as shown in

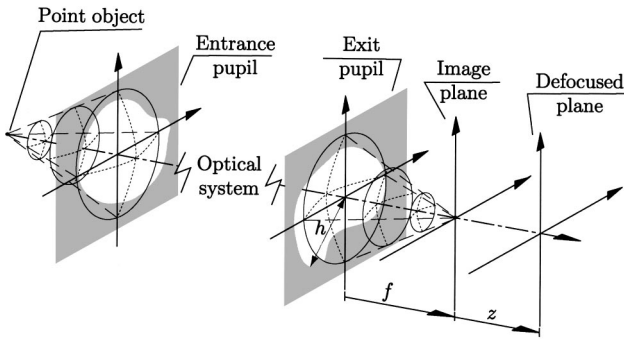


Fig. 1 Schematic representation of the imaging system at issue. The maximum extent of its exit pupil is represented by h ; f is the system focal length.

Fig. 1. The performance of such a system with residual aberrations can be assessed by computing its polychromatic impulse response along the optical axis. This response is characterized by the axial tristimuli values, defined for each axial point as

$$\begin{aligned}
 X(\delta\omega_{20}) &= \int_{\lambda} I(\delta\omega_{20};\lambda) \bar{x}_{\lambda} S(\lambda) d\lambda, \\
 Y(\delta\omega_{20}) &= \int_{\lambda} I(\delta\omega_{20};\lambda) \bar{y}_{\lambda} S(\lambda) d\lambda, \\
 Z(\delta\omega_{20}) &= \int_{\lambda} I(\delta\omega_{20};\lambda) \bar{z}_{\lambda} S(\lambda) d\lambda,
 \end{aligned}
 \tag{1}$$

where $I(\delta\omega_{20};\lambda)$ is the axial monochromatic irradiance PSF, and $\delta\omega_{20}$ is the defocus coefficient defined by (see Fig. 1)

$$\delta\omega_{20} = \frac{-h^2 z}{2f(f+z)}.
 \tag{2}$$

In Eqs. (1) $S(\lambda)$ represents the spectral distribution of the point source, and \bar{x}_{λ} , \bar{y}_{λ} , and \bar{z}_{λ} denote the spectral tristimuli values.¹ These later parameters are considered as the chromatic sensitivity functions of the human eye taken as a receiver, for a given selection of the primary colors. Besides, other polychromatic merit functions such as the chromaticity coordinates and the axial illuminance can be calculated from the tristimuli values along the optical axis in Eq. (1), as is shown in Sec. 3.

For the calculation of the polychromatic merit functions in Eqs. (1), it is necessary to obtain the different monochromatic irradiance PSFs provided by the system for a suitably large number of both wavelengths and axial points in the interval of interest. These axial PSFs are given, according to the Fresnel approximation, by

$$\begin{aligned}
 I(\delta\omega_{20};\lambda) &= \left| \frac{\delta\omega_{20}}{\lambda} \int_0^{2\pi} \int_0^{\infty} \tau(r,\phi) \right. \\
 &\quad \times \exp\left\{ \frac{i2\pi}{\lambda} [\omega(r,\phi;\lambda) + \delta\omega_{20}r^2] \right\} r dr d\phi \Big|^2,
 \end{aligned}
 \tag{3}$$

where $\tau(r,\phi)$ is the pupil function of the system expressed in canonical polar coordinates at the exit pupil plane,¹¹ and $\omega(r,\phi;\lambda)$ is the wave aberration function.

Next we revise the two numerical methods used in this study to compute the monochromatic irradiance PSFs in Eq. (3). In the analysis, we consider systems suffering from SA and LCA, so for those systems, the aberration function is reduced to

$$\omega(r,\phi;\lambda) = \omega_{20}(\lambda)r^2 + \omega_{40}(\lambda)r^4,
 \tag{4}$$

where $\omega_{20}(\lambda)$ and $\omega_{40}(\lambda)$ are the LCA and SA coefficients, respectively. We assume that the chromatic variations of the pupil function are negligible. A unique common feature of both methods is the use of a change of variable $t=r^2$ in Eq. (3) to simplify the numerical computation.^{4,7}

2.1 Hopkins-Yzuel-Calvo (H-Y-C) Method

To evaluate Eq. (3) with the method of Hopkins and Yzuel (modified by Yzuel and Calvo⁴), the integration domain is divided into elementary areas. Each area element is an annular sector defined around its midpoint (t_j, ϕ_k) (note that the first variable is the squared radius). Then the value of the integral is obtained as the sum

$$\begin{aligned}
 I(\delta\omega_{20};\lambda) &= \left| \frac{\delta\omega_{20}}{2\lambda} \sum_{j=1}^J \sum_{k=1}^K \int_{\phi_k-\varepsilon}^{\phi_k+\varepsilon} \int_{t_j-\eta}^{t_j+\eta} \tau(t,\phi) \right. \\
 &\quad \times \exp\left\{ \frac{i2\pi}{\lambda} [\omega_{40}(\lambda)t^2 + \omega_{20}(\lambda)t + \delta\omega_{20}t] \right\} \\
 &\quad \times dt d\phi \Big|^2.
 \end{aligned}
 \tag{5}$$

The amplitude and phase terms inside the integrals in Eq. (5) are expanded in a Taylor series in each area element and only the first order is considered. In this way, closed formulas are achieved in terms of the sampled values over the pupil. By increasing the number of azimuthal and radial samples the accuracy of the calculation can be improved, so the value of the intensity can be obtained with an error lower than a given value. Obviously, this gain in accuracy is associated with an increment of the computation time.

2.2 WDF Method

The monochromatic PSF along the optical axis for an imaging system can also be computed using the WDF obtained from the pupil function of the system. In this case, it is first necessary to express this PSF as a function of a single radial integral by performing the azimuthal average of the pupil function $\tau(t,\phi)$. If we call this function $\tau_0(t)$, Eq. (3) can be expressed as

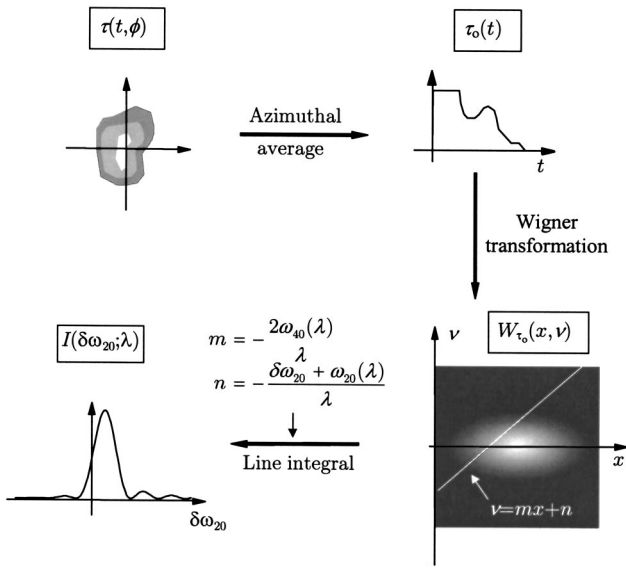


Fig. 2 Summary of the procedure to obtain the PSFs by means of the WDF technique. See the main text for the definitions.

$$I(\delta\omega_{20}; \lambda) = \left| \frac{\delta\omega_{20}}{2\lambda} \int_0^\infty \tau_0(t) \exp\left(\frac{i2\pi}{\lambda} \{[\delta\omega_{20} + \omega_{20}(\lambda)]t + \omega_{40}(\lambda)t^2\}\right) dt \right|^2. \quad (6)$$

It was shown in Ref. 7 that, after a change of variables, this result can also be expressed in terms of the WDF of $\tau_0(t)$, i.e.,

$$I(\delta\omega_{20}; \lambda) = \left(\frac{\delta\omega_{20}}{2\lambda} \right)^2 \int_{-\infty}^{\infty} W_{\tau_0} \left\{ x, -\frac{2\omega_{40}(\lambda)}{\lambda} x - \frac{[\delta\omega_{20} + \omega_{20}(\lambda)]}{\lambda} \right\} dx, \quad (7)$$

where

$$W_{\tau_0}(x, \nu) = \int_{-\infty}^{+\infty} \tau_0\left(x + \frac{x'}{2}\right) \tau_0^*\left(x - \frac{x'}{2}\right) \exp(i2\pi x' \nu) dx'. \quad (8)$$

Figure 2 schematically summarizes the whole procedure to obtain the axial monochromatic irradiance PSFs with this technique. First, from the 2-D pupil function of the system a 1-D azimuthal average is obtained. Then the WDF of $\tau_0(t)$ is computed. Finally, all the axial irradiances are obtained from this single representation by integrating the values of this function along straight lines in the phase-space domain. The slope and the y-intercepts of these lines are given by λ and by the aberration coefficients [see Eq. (7)], which are the variable parameters for the computation.*

*Although the integral in Eq. (6) can be computed as the fast Fourier transform of $\tau_0(t) \exp[i2\pi\omega_{40}(\lambda)t^2/\lambda]$, the rapid oscillations of this function for $\omega_{40} \neq 0$ makes this solution inefficient.

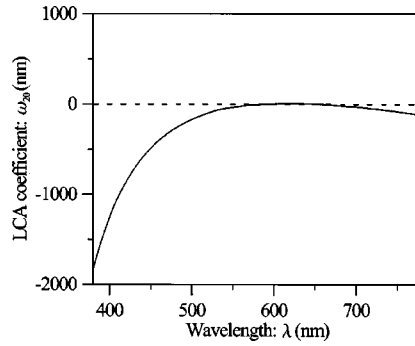


Fig. 3 LCA suffered by the optical systems under test.

As we can see, the accuracy achieved with this method depends basically on the precision in the numerical computation of the WDF $W_{\tau_0}(x, \nu)$. For this calculation, a sampling of the averaged pupil $\tau_0(t)$ is performed and the integral in Eq. (8) is evaluated through a sequence of discrete Fourier transformations. To minimize the aliasing effect inherent to these digital transformations, the averaged pupil is conventionally sampled over an extended domain to include a proper zero-padding.¹²

3 Comparative Study

To compare the performance of both methods, the polychromatic response was computed for several systems with pupils of different shapes, namely, triangular, square, and elliptical. Two different pupils of this last type were considered: pupil A, with a semi-axes ratio 0.5, and pupil B, with a semi-axes ratio 0.75. We assumed that all systems share a focal length $f=1$ m and a Fresnel number $N=200$ for $\lambda=500$ nm. The systems suffered from the LCA shown in Fig. 3 and a constant SA characterized by $\omega_{40}(\lambda)=600$ nm. Both algorithms were implemented in GNU/C programming language, and they were compiled and run in a PC with a Pentium III 800-MHz processor. The operating system used was GNU/Linux (v. 2.2).

As mentioned, a large number of the monochromatic PSFs provided by the system [Eq. (2)] must be computed to obtain its polychromatic response. To get a first impression of the behavior of both algorithms, we estimated the accumulated CPU time t_{CPU} they required to compute the successive monochromatic irradiances for 501 axial points in the interval $-2.5 \mu\text{m} \leq \delta\omega_{20} \leq 2 \mu\text{m}$ around the image plane. This t_{CPU} depends on the sampling density used in each method. Obviously, as the sampling density increases, the accuracy of the results obtained by both methods becomes higher. Regarding the H-Y-C method, to simplify this analysis, we considered the same number of radial and azimuthal intervals over the pupil [i.e., $J=K$ in Eq. (5)] as a typical choice for the sampling. On the other hand, to ensure the antialiasing effect of the zero-padding method in the WDF technique, we considered for the pupil function an extended domain that covers twice of its width.

To fix the comparison conditions, we chose in both cases the minimum number of sampling points that provide a maximum mean error below 0.15% throughout the full

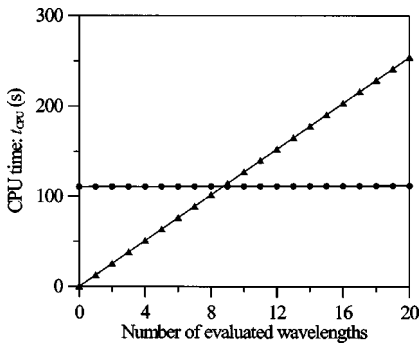


Fig. 4 Computation time (for a fixed accuracy) versus the number of monochromatic irradiances evaluated, for an axial interval $-2.5 \mu\text{m} \leq \delta\omega_{20} \leq 2 \mu\text{m}$. Triangular and circular symbols correspond to H-Y-C and WDF techniques, respectively.

range of considered axial positions. This mean error was calculated from the formula

$$\bar{\varepsilon}_\lambda (\%) = 100 \frac{\int_{\delta\omega_{20} \min}^{\delta\omega_{20} \max} |I(\delta\omega_{20}; \lambda) - \bar{I}(\delta\omega_{20}; \lambda)| d\delta\omega_{20}}{\int_{\delta\omega_{20} \min}^{\delta\omega_{20} \max} \bar{I}(\delta\omega_{20}, \lambda) d\delta\omega_{20}}, \quad (9)$$

where $\bar{I}(\delta\omega_{20}; \lambda)$ is the common asymptotic value of $I(\delta\omega_{20}; \lambda)$ obtained from a very large number of sampling points with any of the two methods. The corresponding

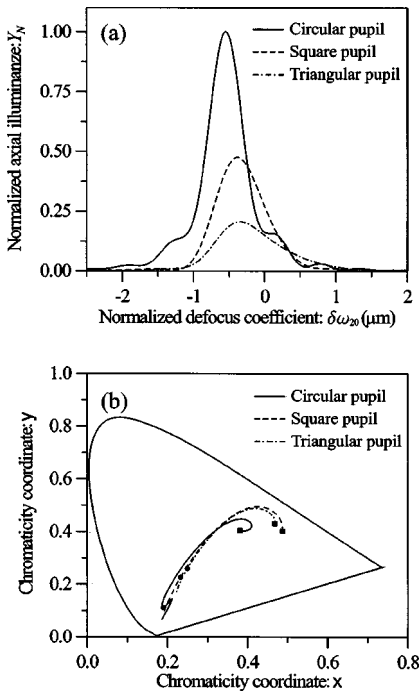


Fig. 5 (a) Normalized axial illuminance and (b) axial chromaticity diagram for $-1.5 \mu\text{m} \leq \delta\omega_{20} \leq 0.5 \mu\text{m}$, obtained with triangular and square apertures compared with the results for a circular pupil. In (b), the circles and squares indicate the axial points given by $\delta\omega_{20} = 0$ (image plane) and $\delta\omega_{20} = -1.5 \mu\text{m}$, respectively.

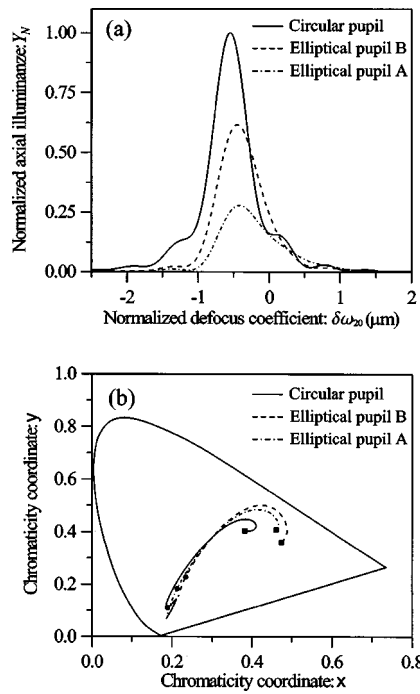


Fig. 6 Same as in Fig. 5 for elliptical pupils.

values of t_{CPU} for a square pupil and wavelengths ranging in the interval $380 \text{ nm} \leq \lambda \leq 780 \text{ nm}$ are presented in Fig. 4. It is clear that the accumulated time to compute the first nine monochromatic PSFs is lower for the H-Y-C method. In fact, the WDF method needs a bias time (estimated as 110 s in the case at issue) to compute the azimuthal average of the pupil and its WDF. As the number of computed integrals increases, the computation time linearly increases with both methods, but the slope with the WDF technique is much lower. Therefore, we can conclude that from a few monochromatic PSFs on, this method becomes progressively more efficient than the classical H-Y-C technique.

To assess the polychromatic behavior of the different pupil functions under study, we computed a conventional set of merit functions derived from the tristimuli values, namely, the normalized axial illuminance $Y_N(\delta\omega_{20})$, and the chromaticity coordinates¹ x and y , defined as

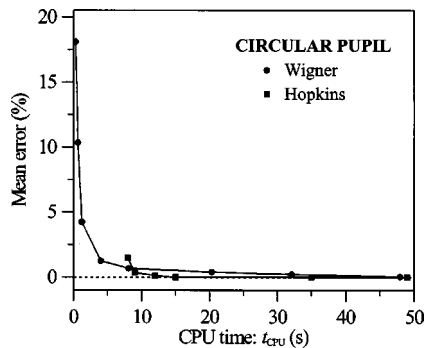


Fig. 7 Mean error versus computation time for the normalized axial illuminance provided by the system with a circular pupil.

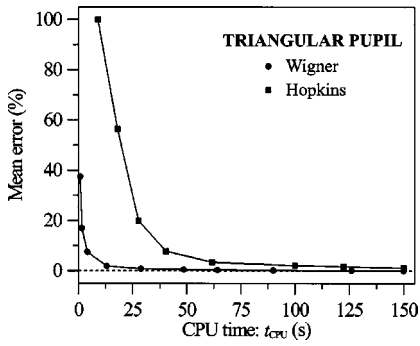


Fig. 8 Same as Fig. 7 for a triangular pupil.

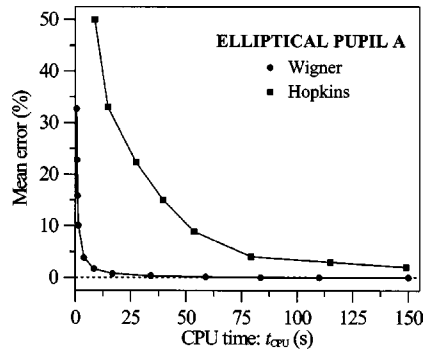


Fig. 10 Same as Fig. 7 for elliptical pupil A (semiaxes ratio 0.5).

$$Y_N(\delta\omega_{20}) = \frac{Y(\delta\omega_{20})}{\int_{\lambda} (1/\lambda^2) \bar{y}_{\lambda} S(\lambda) d\lambda},$$

$$x(\delta\omega_{20}) = \frac{X(\delta\omega_{20})}{X(\delta\omega_{20}) + Y(\delta\omega_{20}) + Z(\delta\omega_{20})}, \quad (10)$$

$$y(\delta\omega_{20}) = \frac{Y(\delta\omega_{20})}{X(\delta\omega_{20}) + Y(\delta\omega_{20}) + Z(\delta\omega_{20})}.$$

The results of the computation of these merit functions for the different pupils at issue are shown in Figs. 5 and 6. The spectral sensitivity functions used in the computation of the axial tristimuli values correspond to those associated with Commission Internationale de l'Éclairage (CIE) 1931 standard observer. For the spectral distribution of the source we used the standard illuminant C. The integrals in Eq. (1) were numerically evaluated for 401 equally spaced wavelengths in the range $380 \text{ nm} \leq \lambda \leq 780 \text{ nm}$, for the same axial interval used in Fig. 4. Note that these figures were computed with an accuracy such that the difference between both methods in each evaluated monochromatic irradiance was lower than 0.5%. In this way, both techniques lead to undistinguishable results for Figs. 5 and 6.

We also estimated the mean error that affects the normalized axial illuminance as a function of the computation time required with both methods. This mean error was computed through a formula similar to the proposed one in Eq. (9), namely,

$$\bar{\varepsilon}(\%) = 100 \frac{\int_{\delta\omega_{20 \min}}^{\delta\omega_{20 \max}} |Y_N(\delta\omega_{20}) - \bar{Y}_N(\delta\omega_{20})| d\delta\omega_{20}}{\int_{\delta\omega_{20 \min}}^{\delta\omega_{20 \max}} \bar{Y}_N(\delta\omega_{20}) d\delta\omega_{20}}, \quad (11)$$

where $\bar{Y}_N(\delta\omega_{20})$ is the common asymptotic value of $Y_N(\delta\omega_{20})$ for a high sampling rate with both methods. As in the previous analysis, in the H-Y-C technique, we assumed equal sampling density in radial and azimuthal coordinates over the pupil of the system. For the WDF technique, we used the same zero-padding method considered in the preceding monochromatic analysis.

As expected, a considerable reduction in the computation time of the polychromatic axial response is achieved with the WDF method. This result is shown in Figs. 7–11. As we can see from these figures, the WDF method always takes less computation time to achieve the same value of the mean error except in the case of the circular pupil. Considering triangular and square pupils as polygonal approaches to the circular aperture, and elliptical pupils as deformations of the circular pupil, we can assert that, as the pupil shape departs from the perfectly circular pupil, for a given degree of accuracy, the WDF method is faster than the H-Y-C technique. This conclusion is based on the comparison of the results provided in Figs. 8 and 9 (the square pupil can be considered to be closer to the circular aperture than the triangular one) and in Figs. 10 and 11 (as the semiaxes ratio approaches unity, the aperture tends to the perfectly circular pupil).

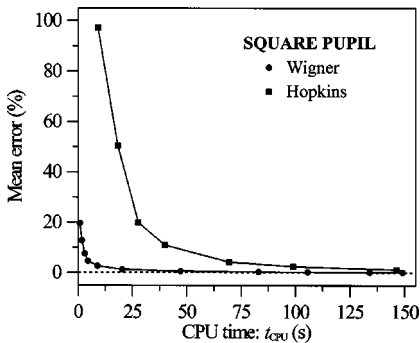


Fig. 9 Same as Fig. 7 for a square pupil.

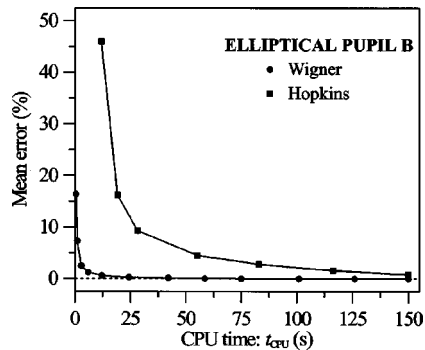


Fig. 11 Same as Fig. 7 for elliptical pupil B (semiaxes ratio 0.75).

4 Conclusions

An assessment of a new method for the numerical computation of the axial impulse response of an imaging system was presented. A comparative study with the H-Y-C classical method was performed to test the efficiency in the computation of the polychromatic response provided by imaging systems suffering from longitudinal chromatic aberration and spherical aberration. Several pupil functions useful in different technological applications were investigated including square, triangular, and elliptical pupils. It was found that to obtain a given degree of accuracy, the new method is more efficient than the classical technique when the pupil of the system is not circular. This fact can be explained taking into account that in the new method, all the monochromatic irradiances are obtained from a single 2-D phase-space function, while in the classical method the entire calculation must be repeated for each axial position, wavelength, and aberration function. Although the calculation of the WDF must be taken into account in the computation time, the ratio of this contribution to the total time, when a high number of axial positions are involved is less and less important as the number of monochromatic components increases.

Acknowledgments

This research has been supported by the Plan Nacional I +D+I (Grant No. DPI 2000-0774), Ministerio de Ciencia y Tecnología, Spain.

References

1. M. J. Yzuel and J. Santamaría, "Polychromatic optical image. Diffraction limited system and influence of the longitudinal chromatic aberration," *Opt. Acta* **22**, 673–690 (1975).
2. M. J. Yzuel, J. C. Escalera, and J. Campos, "Polychromatic axial behavior of axial apodizing and hyperresolving filters," *Appl. Opt.* **29**, 1631–1641 (1990).
3. H. H. Hopkins and M. J. Yzuel, "The computation of diffraction patterns in the presence of aberrations," *Opt. Acta* **20**, 157–182 (1970).
4. M. J. Yzuel and F. Calvo, "Point spread function calculation for optical systems with residual aberrations and non-uniform transmission pupil," *Opt. Acta* **30**, 233–242 (1983).
5. J. J. Stamnes, B. Spjelkavik, and H. M. Pedersen, "Evaluation of diffraction integrals using local phase and amplitude approximations," *Opt. Acta* **30**, 207–222 (1983).
6. L. A. D'Arcio, J. J. M. Braat, and H. J. Frankena, "Numerical calculation of diffraction integrals for apertures of complicated shape," *J. Opt. Soc. Am. A* **11**, 2664–2674 (1994).
7. G. Saavedra, W. D. Furlan, E. Silvestre, and E. E. Sicre, "Analysis of the irradiance along different paths in the image space using the Wigner distribution function," *Opt. Commun.* **139**, 11–16 (1997).
8. W. D. Furlan, G. Saavedra, E. Silvestre, P. Andrés, and M. J. Yzuel, "Polychromatic axial behavior of aberrated optical systems: Wigner distribution function approach," *Appl. Opt.* **36**, 9146–9151 (1997).
9. G. P. Karman, G. S. McDonald, G. H. New, and J. P. Woederman, "Laser optics: Fractal modes in unstable resonators," *Nature (London)* **402**, 138 (1999).
10. P. Nesenson and C. Papaliolios, "Detection of earth-like planets using apodized telescopes," *Ap. J.* **548**, L201–L205 (2001).
11. H. H. Hopkins, *Wave Theory of Aberrations*, Oxford University Press, Oxford (1950).
12. W. H. Press, B. P. Flannery, S. A. Teukolsky, and W. T. Vetterling, *Numerical Recipes in Pascal*, Cambridge University Press, New York (1989).



Walter D. Furlan received his MS and PhD degrees in physics from the University of La Plata in 1984 and 1988, respectively. From 1984 to 1990 he performed research work at the Centro de Investigaciones Ópticas (CIOp), Argentina. In 1990 he joined the Optics Department of the University of Valencia, Spain, where he is currently a professor of optics. His research interests include image processing using phase-space representations, optometry, and physiological optics.

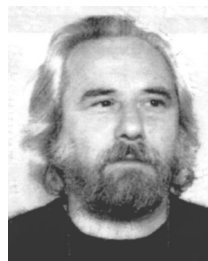


Genaro Saavedra received his BS and PhD degrees in physics in 1990 and 1996, respectively, from the Universitat de València, Spain, where he is currently an associate professor. His research interests are optical diffraction, phase-space representation of scalar optical fields, and ultrashort light pulse propagation.

Enrique Silvestre: Biography and photograph not available.



Juan A. Monsoriu received his BS degree in physics in 1998 and his MS degree in optics in 2000 both from the Universidad de Valencia (UV), Spain. Since 2000 he has been an assistant professor with the Department of Applied Physics, Universidad Politécnica de Valencia (UPV), Spain, where he is involved with information and communication technologies applied to the transmission of scientific knowledge. He is also currently working toward



his PhD degree in physics in the Department of Optics at UV. His main research interests are modal methods for the design of inhomogeneous waveguides and dielectric resonators.

José D. Patrignani received his engineer and master in engineering degrees from the Universidad Nacional del Sur, Bahía Blanca, Argentina, in 1987 and 2000, respectively. Since 1994 he has performed research in the Departamento de Física, Universidad Nacional del Sur, where he is currently an assistant professor of electromagnetism and optics. His research interests include image processing and optical methods in experimental mechanics.